Neuromol Med (2008) 10:24–39
DOI 10.1007/s12017-007-8020-z

ORIGINAL PAPER

Chronic Exposure to Dietary Sterol Glucosides is Neurotoxic to Motor Neurons and Induces an ALS–PDC Phenotype

R. C. Tabata · J. M. B. Wilson · P. Ly · P. Zwiegers · D. Kwok · J. M. Van Kampen · N. Cashman · C. A. Shaw

Received: 25 June 2007 / Accepted: 2 November 2007 / Published online: 15 January 2008

Abstract Epidemiological studies of the Guamanian variants of amyotrophic lateral sclerosis (ALS) and parkinsonism, amyotrophic lateral sclerosis–parkinsonism dementia complex (ALS–PDC), have shown a positive correlation between consumption of washed cycad seed flour and disease occurrence. Previous in vivo studies by our group have shown that the same seed flour induces ALS and PDC phenotypes in out bred adult male mice. In vitro studies using isolated cycad compounds have also demonstrated that several of these are neurotoxic, specifically, a number of water insoluble phytosterol glucosides of which β-sitosterol β-D-glucoside (BSSG) forms the largest fraction. BSSG is neurotoxic to motor neurons and other neuronal populations in culture. The present study shows that an in vitro hybrid motor neuron (NSC-34) culture treated with BSSG undergoes a dose-dependent cell loss. Surviving cells show increased expression of HSP70, decreased cytosolic heavy neurofilament expression, and have various morphological abnormalities. CD-1 mice fed mouse chow pellets containing BSSG for 15 weeks showed motor deficits and motor neuron loss in the lumbar and thoracic spinal cord, along with decreased glutamate transporter labelling, and increased glial fibrillary acid protein reactivity. Other pathological outcomes included increased caspase-3 labelling in the striatum and decreased tyrosine-hydroxylase labelling in the striatum and substantia nigra. C57BL/6 mice fed BSSG-treated pellets for 10 weeks exhibited progressive loss of motor neurons in the lumbar spinal cord that continued to worsen even after the BSSG exposure ended. These results provide further support implicating sterol glucosides as one potential causal factor in the motor neuron pathology previously associated with cycad consumption and ALS–PDC.

Keywords ALS · Parkinsonism · BSSG · Guam · Environmental toxicity · Etiology · ALS-PDC

R. C. Tabata · P. Ly · C. A. Shaw (✉)
Department of Experimental Medicine,
University of British Columbia, Rm 386, 828 W.10th Ave,
Vancouver, BC, Canada V5Z1L8
e-mail: cashawlab@gmail.com

J. M. B. Wilson · C. A. Shaw
Program in Neuroscience, University of British Columbia,
Vancouver, BC, Canada

P. Zwiegers · D. Kwok · C. A. Shaw
Department of Ophthalmology and Visual Sciences,
University of British Columbia, Vancouver, BC, Canada

J. M. Van Kampen
Department of Neuroscience, Mayo Clinic,
Jacksonville, Fl, USA

N. Cashman
Department of Medicine, University of British Columbia,
Vancouver, BC, Canada

C. A. Shaw
Department of Physiology, University of British Columbia,
Vancouver, BC, Canada

Introduction

The primary causal factor(s) for the neurodegenerative disease amyotrophic lateral sclerosis–parkinsonism dementia complex (ALS–PDC) has eluded investigators since the disease was first characterized by Kurland and colleagues in the 1950s (see Kurland and Molgaard 1982, for a summary). Then, as now, the strongest epidemiological link was to local consumption by the native

Chamorro people of the starchy gametophyte of the indigenous cycad tree (*Cycas micronesica*) (Whiting 1963; Kurland 1988; Borenstein et al. 2007; Galasko et al. 2007).

Based on the epidemiological evidence for cycad neurotoxity leading to ALS–PDC, we conducted a series of in vivo studies demonstrating that washed cycad flour prepared in a manner consistent with native Chamorro practice produces behavioral deficits and CNS pathologies in mice mimicking many aspects of the human disease (Wilson et al. 2002, 2004a, b, 2005b; Schulz et al. 2003). The cycad flour used had been 'washed' numerous times and contained nil-to-trace amounts of the previously suspected cycad toxins, notably the free amino acids β-N-methylamino-L-alanine (BMAA) and β-N-oxalylamino-L-alanine (BOAA), or the amino sugar cycasin and its aglycone, methylazoxymethanol (MAM) (Wilson et al. 2002). Earlier studies by Spencer et al. (1987) had demonstrated some neurotoxic effects of BMAA in vivo in macaque monkeys following exposure to BMAA by gavage at extremely high concentrations. These outcomes, however, did not resemble the pathology of ALS–PDC. In addition, the results in monkeys were not confirmed either by us (Cruz-Aguado et al. 2006) or others (Perry et al. 1989) in mice. Recently, Murch et al. (2004) have suggested that BMAA may exist in a protein-associated "bound" form that is magnified up the food chain. Evidence for either BMAA incorporation into protein or its actual toxic impact, however, is lacking: In the first case, apart from the claims of these investigators, there is no evidence that such bound forms of BMAA or other plant free amino acids exist. In regard to BMAA toxicity, recent studies have shown that even direct injection of high concentrations of BMAA into brain had no effects on the target neuron populations (Buenz and Howe 2007).

In contrast to BMAA, BOAA ingestion in animals and humans could induce neurodegeneration in a condition called neurolathyrism, but this disorder does not resemble ALS–PDC (Ross et al. 1989). Similarly, neither cycasin nor MAM give ALS–PDC-like phenotypes (for a review, see Kurland 1972).

Based on all of the above studies, our working hypothesis has been that a previously uncharacterized water-insoluble neurotoxin(s) in washed cycad flour is responsible for the human disease and for the similar outcomes in our cycad-treated mice. In a series of parallel in vitro assays, we isolated the neurotoxic fractions from washed cycad seed "chips" (Khabazian et al. 2002). The most toxic fraction was found to contain a water insoluble mixture of phytosterol β-D-glucosides, including β-sitosterol β-D-glucoside (abbreviated here as BSSG, the largest fraction, MW = 576 g/mol), stigmasterol β-D-glucoside, and campesterol β-D-glucoside. HPLC analyses had shown that BSSG concentrations range from about 20 μg/g to 1,340 μg/g (Marler et al. 2005).

The variation in the concentration of BSSG appears to depend on several factors, including the region harvested and season. Seed maturity appears to be the most crucial factor with younger seeds having higher concentrations by up to several orders of magnitude (Marler et al. 2006). Similar variations for stigmasterol glucoside and other phytosterol glucosides have also been measured (Marler et al. 2005).

In all higher plants, sterols occur free as esters, as β-D-glucosides, and as their 6-O'-esters in small, but readily identifiable amounts (Grunwald 1980). Phytosterols such as sitosterol and stigmasterol occupy the exofacial leaflet of the cell membrane. In contrast, cholesterol and its esters in plant and animal cells readily partition into the cytofacial leaflet and are important membrane components (Grunwald 1980). The cellular localization of these sterols in bilamellar cell membranes of both plants and animals may thus have important implications for membrane conformation and permeability.

The roles of the various phytosterol glucosides are not well understood. To some extent they may generally share with sterols a role in the maintenance of cell membrane structure (Pegel 1997). Due to the hydrophilicity of the glucose moiety, these molecules may have surface-active binding sites and properties (Folmer 2003), similar to better-known phytosterol glucosides such as ouabain and digitalin (Nesher et al. 2007). For most phytosterol glucosides binding sites have not been identified.

In support of our preliminary data suggesting neurotoxic actions of cycad's sterol glucosides, other sterols and sterol glucosides have been shown to exhibit toxic properties in animal cells (see Ly et al. 2007 for references). In contrast, cholesterol glucoside has been implicated as playing a primary role in the early stages of stress-induced signal transduction in various animal cells, including cultured human fibroblasts (Murakami-Murofushi et al. 1997; Kunimoto et al. 2000, 2002). The cumulative data thus clearly demonstrate that sterol glucosides from plants or animal cells are not uniform in their actions and may span the range of actions from protective to toxic.

Our preliminary in vitro studies had shown that cycad-derived BSSG and other phytosterol glucosides, as well as synthetic BSSG and cholesterol glucoside (CG), were acutely toxic to cortical slices and primary cortical cultures in micromolar concentrations with at least part of their action due to glutamate release *prior* to cell death. Exposure of neural cells to these sterol glucosides also induced a significant up-regulation of protein kinases including PKC and CDK2 and CDK5 (Khabazian et al. 2002). Significantly, in regard to a possible link to ALS–PDC and the neurofibrillary tangles which are a ubiquitous feature of the disease, BSSG also induced increased hyperphosphorylated tau expression in neurons (Khabazian et al. 2002) and in

NSC-34 motor neuron hybrids (Ly et al. 2007). Chronic treatment of organotypic slice preparations at nanomolar concentrations showed that BSSG induced cell death in a dose-dependant manner in the spinal cord, hippocampus, and substantia nigra (SN) slice preparations (Wilson et al. 2005c; K. Andreassen, C. Mathews; S. Jafri, personal communications, respectively).

The identification of BSSG as one cycad compound potentially causal to the forms of neural degeneration leads to a testable hypothesis: BSSG alone or in combination with other cycad sterol glucosides will produce essentially the same neuropathological outcomes as cycad seed flour. The following studies were designed to test this hypothesis: We fed BSSG (incorporated into mouse chow pellets) to two strains of adult male mice over a prolonged period of time ranging from 10 to 15 weeks. Detailed analyses of behavioral, morphological, and biochemical outcomes were followed temporally with an emphasis on the emergence of ALS–PDC-like features in two CNS regions associated with the disease, specifically motor neurons of the lumbar and thoracic spinal cord and dopamine containing neurons of the nigro-striatal system.

Materials and Methods

In vitro Experiments

Cell Culture Preparation

The mouse-derived motor neuron-like cell line, NSC-34, was cultured in a Dulbecco's modified Eagle's medium (DMEM) supplemented with 10% fetal bovine serum and 2 mM L-glutamine. NSC-34 cells were maintained in a humidified 5% CO_2 atmosphere at 37°C. For each experiment, cells were seeded at 2×10^4 cells/mm^2.

β-Sitosterol β-D-glucoside (BSSG) Treatment and Cell Death Assay

The NSC-34 cells were grown on 24-well collagen-coated plates (Corning Transwell-col membrane, 6.5 mm diameter, 0.4 μm pore, PTFE, sterile, from Sigma-Aldrich, UK) and treated with increasing doses of pure synthetic BSSG (0.1–100 μM). BSSG was dissolved in pure DMSO and diluted in DMEM. The maximum percentage of DMSO used in the experiments was 0.5%. Cell viability of the NSC-34 cells after BSSG treatment was determined by the trypan blue exclusion assay after 3 days of BSSG treatment. Cell death was expressed as the number of dead cells divided by the total number of cells counted.

Cell Lysate Preparation and Western Blot Analysis

At the end of each treatment, cells were washed once with ice-cold phosphate-buffered saline (PBS; Sigma-Aldrich) and lysed in a homogenizing buffer containing 20 mM MOPS, 5 mM EDTA, 2 mM EGTA, 30 mM NaF, 1 mM PMSF, 1 mM $NaVO_3$, 20 mM beta-glycerophosphate, 0.5% Triton X-100 (polyethylene glycol *p*-tert-octylphenyl ether, Fisher BioReagents, Fisher Scientific, Pittsburgh, PA), and protease inhibitor cocktail tablet (Roche Molecular Biochemicals, Indianapolis, IN). Cell lysates were sonicated 15 times and centrifuged at 12,000 rpm for 30 min at 4°C. Protein concentration was determined using a commercial bicinchoninic acid (BCA) protein concentration kit (Peirce, Rockford, IL).

About 10 μg of cell lysates were boiled in sample buffer and resolved on a 10% sodium dodecyl sulfate polyacrylamide gel, followed by transferring the resolved proteins onto a nitrocellulose membrane. The membranes were blocked for 1 h with 1% bovine serum albumin in 0.1% TBS-Tween 20 (Sigma-Aldrich) at room temperature and incubated with specific antibodies at 4°C for up to 18 h. Primary antibodies recognizing HSP70 (1:2,000) and the heavy subunit of neurofilament (1:1,000) were used. Secondary HRP-conjugated antibodies were used to detect specific bands followed by enhance chemiluminescence light reaction (Amersham).

In vivo Experiments

Experiment 1: Is BSSG Neurotoxic In vivo?

Animals. Five to seven-month-old male CD-1 mice were purchased from Charles River (Wilmington, MA). CD-1s were selected for the initial BSSG neurotoxicity experiment as our laboratory has demonstrated the effects of cycad flour consumption on CNS pathology in this same strain (Wilson et al. 2003, 2004a, b, 2005b). Thirty-one mice were randomly divided into two groups (15 controls; 16 experimental). All animals were housed singly in a room maintained at 22°C in a 12/12 h light cycle.

Feeding of BSSG. Gram quantities of BSSG were synthesized on a contract basis by the Department of Chemistry, University of British Columbia. In short, a multi-step process converted unglycosylated sterols (*β*-sitosterol or cholesterol) into BSSG or cholesterol *β*-D-glucoside, respectively. Synthesized compounds were characterized using NMR (^{1}H and ^{13}C) and high-resolution mass spectrometry (HRMS). A purity of at least 95% was verified by HPLC. BSSG was mixed with ground up Purina Chow mouse pellets (Mouse Diet^{TM}, Purina) to create the experimental pellet at the desired concentrations of BSSG/

pellet. In the studies using CD-1 mice, the dose in the experimental group was 1,000 μg of BSSG/day. Treated pellets were placed in the feeding tray each morning before the addition of regular mouse chow (*ad libitum*). Any uneaten experimental pellets were weighed and recorded. In general, all of the mice in the BSSG group routinely ate the entire pellet. Control mice were fed only normal mouse chow. BSSG feeding was conducted daily for 15 weeks and mice were behaviorally monitored for an additional 17 weeks prior to sacrifice.

Experiment 2: Dose Dependence of BSSG-induced Neurodegeneration

Animals. The strain-dependency of possible BSSG effects was assessed using 3-month-old male C57/BL6 mice purchased from Taconic (Germantown, NY). Forty-four mice were randomly divided into four groups (14 controls; 10 for each of the experimental groups (see below)). All animals were housed singly in a room maintained at 22°C in a 12/12 h light cycle.

Feeding of BSSG. Daily doses of 10, 100, or 1,000 μg BSSG were fed to the separate experimental groups starting at 5 months of age. These dosages were chosen to show the effect of BSSG feeding at concentrations below, near, and above those previously described as extant in cycad flour (Wilson et al. 2002). Feeding was conducted daily for 10 weeks. An additional 2 weeks of behavioral testing was conducted after BSSG feeding ended (total 12 weeks of testing) to allow blood sterol content to become normalized (Sanders et al. 2000; Miettinen et al. 1983). At this stage, half the mice were sacrificed. The remaining mice were sacrificed 5 months later in order to determine if BSSG had long-term progressive pathological effects similar to the effects observed with cycad feeding (Wilson et al. 2002). Other aspects of this study were as described in Experiment 1.

The following methods were common for both in vivo studies.

Blood Collection and Preparation. Blood collection (via tail bleed) was completed in both in vivo experiments. In Experiment 1, blood was taken before and during BSSG feeding (week 8); in Experiment 2, blood was collected before and during BSSG feeding (week 10). The tail tip (2 mm) from each mouse was cut off with a sterile scalpel to sever the lateral vein. Serum sterol glucoside levels, presumably including both exogenous phytosterol glucoside and endogenous CG, in plasma samples were determined after thin layer chromatography (TLC). About 100 μl aliquots of thawed plasma were transferred to microcentrifuge tubes with 250 μl of acetonitrile and centrifuged at 3,000 rpm for 3 min to precipitate the pellet. The supernatant was transferred and extracted with 500 μl chloroform. The mixture was vortexed (Vortex Genie-2, Scientific Industries, Inc., Bohemia, NY) and spun at 3,000 rpm for 3 min. The upper aqueous layer was transferred and extracted for a second time with 500 μl chloroform and for a third time with 500 μl chloroform/methanol (2:1 v/v). The combined chloroform and chloroform/methanol extracts were transferred to a new vial and dried under a stream of nitrogen. The sample residue was dissolved in 300 μl of reconstituting solvent (20 ml of dichloromethane/methanol (1:1 v/v) + five drops of pyridine) before TLC application.

HPLC. About 10 μl of each of sample extract and a standard amount of BSSG was injected into the HPLC system (Agilent HP 1050 equipped with an Agilent Zorbax Eclipse XDB-C18 column) and separated in isocratic mode during a run time of 30 min using methanol/acetonitrile (80:20) (30°C; 0.5 ml/min). UV detection was at 205 nm. The relative retention time and the peak response were calculated by the Agilent ChemStation Software (Version A.09.01) and used to identify and quantify the corresponding BSSG peak in the sample chromatograms.

Behavioral Tests of Motor Function. In all behavioral experiments, the mice were tested singly between 10 a.m. and 5 p.m. The testing sequence of mice was randomized across groups. The experimental group to which each animal belonged was unknown to the observer at the time of behavioral recording.

Leg Extension. The leg extension reflex test was used as a measure of motor neuron dysfunction (Barneoud and Curet 1999). We altered this test to discriminate more subtle behaviors, employing a scale from 0 to 4 based on the response shown by the mouse. 4: Complete extension of both legs (normal). 3: Two legs extended with some tremors and/or punching of one leg. 2: One leg extended, 1 retracted, or tremors in both legs. 1: One leg retracted and tremors in the other leg. 0: Both legs retracted. Leg extension was measured three times per week. This scaled test was designed to show the progressive loss of function as the normal reflex usually deteriorated progressively to tremor and then to total retraction.

Open Field. Mice were placed in a round open field (2 m diameter) for 5 min and movements were recorded using a video camera to measure exploratory behavior (spontaneous motor activity) (Karl et al. 2003) as well as possible stress response (i.e., defensive burying or thigmotaxis). Videos were viewed on a TV screen with a circular grid overlaid and grid crossings were recorded. Three trials were conducted during weeks 24, 26 and 28.

Rotorod. The rotorod was used to test general motor function (Gerlai et al. 1996; Gerlai and Roder 1996) and

motor learning (Welsh et al. 2005). The time that a mouse could remain walking on a rotating axle (3.6 cm diameter; speed of rotation: 16 rpm) without either falling or clenching onto the axle was measured. Each mouse was tested for a maximum of 160 s (Barneoud et al. 1997) twice per week.

Paw Print Analysis: In order to examine hind limb stepping patterns during forward locomotion, mice were required to traverse a straight, walled runway. Stride length was determined as per previously described protocols (Wilson et al. 2002, 2003, 2004a, b, 2005b).

Wire Hang: Neuromuscular strength was tested by the wire hang (Wilson et al. 2003, 2004a, b, 2005b) in which mice were placed on a wire-cage lid that was turned upside down (180°) over a soft surface and the latency to fall recorded (maximum of 60 s).

Histological/Morphological Measurements

At the various times of sacrifice, all animals were anaesthetized with halothane and perfused via cardiac puncture with chilled PBS and 4% paraformaldehyde (PFA). Spinal cord and brain samples were removed and immersed in 4% PFA for 2 days, cryoprotected in 20% sucrose 0.5% sodium azide in 0.01 M PBS solution, pH 7.4 for 1 day, and then stored frozen at −80°C until sectioning for immunohistology on a Hacker-Bright motorized cryostat. Spinal cords and brains were serially sectioned at 20 and 30 μm, respectively. Spinal cord and mouse brain sections were sectioned in the coronal plane (Wilson et al. 2002, 2003). Immunohistochemistry for any particular assay was performed at the same time for sections for all animals in either of the two studies. Microscopy of the stained sections and recording of the level of labelling was conducted by observers blind to the identity of the mice.

Activated caspase-3 (Promega, Madison, WI; Iba-1 (ionized calcium-binding adaptor molecule-1, Abcam, Cambridge, MA), glial fibrillary acidic protein (GFAP, rat monoclonal antibody, Calbiochem, San Diego, CA), and choline acetyl transferase (ChAT), (Chemicon International; VES Labs, Inc., Tigard, OR) levels were identified by immunohistology (Schulz et al. 2003; Wilson et al. 2005b). Slide-mounted sections were incubated in PBS-blocking solution (1% BSA and 0.3% Triton X-100 in PBS) for 2 h and then with the primary antibody (Casp-3 1:250, Iba-1 1:500, GFAP 1:100, and ChAT 1:100) overnight at 4°C. Sections were rinsed and incubated with the corresponding fluorescent secondary antibodies (AlexaFluor 546 IgG 1:200; AlexaFluor 546 1:200; AlexaFluor 488 1:200; AlexaFluor 555 1:200 obtained from Invitrogen Molecular Probes, Eugene, OR) for 2 h.

Proliferating cell nuclear antigen (PCNA) was used to assess neurogenesis. Sections were pretreated with 50% formamide/280 mM, incubated in 2 M HCl at 37°C for 30 min, and rinsed in 0.1 M boric acid (pH 8.5) for 10 min at room temperature. Sections were incubated in 1% H_2O_2 in phosphate buffered saline for 15 min, in blocking solution (3% goat or donkey serum/0.3% Triton X-100/Tris-buffered saline [TBS]) for 1 h at room temperature, followed by the primary antibody, PCNA (1:1,000, Santa Cruz), at 4°C overnight. In between steps, sections were washed for 3 × 10 min in TBS. Mounting medium containing DAPI (4′,6-diamidino-2-phenylindole, Vector laboratories, Inc., Burlingame, CA) was used to stain cell nuclei, and slide-mounted sections were examined by fluorescent microscopy.

Labelling of dopaminergic neurons in brain sections was identified by antibodies for tyrosine hydroxylase (Morrow et al. 2001). Sections were incubated in blocking serum for 2 h then with the primary antibody (rabbit anti-tyrosine hydroxylase, 1:500) for 3 h at room temperature. Sections were rinsed and incubated in biotinylated goat anti-rabbit IgG (1:100; Vector laboratories Inc., Burlingame, USA) for 30 min at room temperature, then visualized using the ABC method (Vectastain Elite ABC kit, Vector Laboratories Inc.). For quantification, images of spinal cord sections, striatum, or SN were captured with a focal high performance CCD camera and NIH Scion imaging software to measure density levels of antibody labelling. Between 6 and 12 sections from each mouse were measured.

Astrocytic glutamate transporters (GLT) were identified using antibodies for GLT-1B (Reye et al. 2002; Wilson et al. 2003). Sections were incubated in blocking solution for 2 h followed by incubation with the primary antibody (GLT-1B raised in rabbit, 1:1,000) for 4 days at 4°C. Sections were rinsed and incubated in biotinylated goat anti-rabbit IgG (1:100; Vector laboratories Inc., Burlingame, USA) for 2 h, followed by visualization using the ABC method (Vectastain Elite ABC kit, Vector Laboratories Inc.). For quantification, images of spinal cord sections and other CNS regions were obtained with a focal high performance CCD camera analyzed using NIH Scion imaging software to measure density levels of the antibody labelling. Several sections ($n = 5$–6) from each mouse were used.

Microscopy. Microscopy and all photomicrographs from mouse sections were captured using a Motic B5 Professional Series 3.0 (Motic Instruments Inc., Richmond, ON) and Zeiss Axiovert 200 M (Carl Zeiss Canada Limited, Toronto, ON). DAPI labelling (blue fluorescence) was visualized with a 359/461 nm absorption/emission filter. FITC was visualized using a 490,494/520 nm filter. Alexa Fluor 546™ (red

fluorescence) and rabbit IgG DuoLuX^{TM} (red fluorescence) were visualized with a 556,557/572,573 nm filter. During quantitation at 40× magnification, two images were captured per lumbar cord section (i.e., ventral left and ventral right). All 40× images were 350 × 275 μm in dimension. Images were captured using AxioVision 4.3 software. Data were analyzed using Motic B5 Professional, Motic Images Advanced 3.0 and Zeiss Axiovert Zoom Axiovision 3.1 with AxioCam HRM.

To count spinal motor neurons, lumbar and thoracic spinal cord sections were stained with cresyl violet. The ventral horn motor neurons were counted at 40× magnification with parallel sweeps of the microscope stage. Count estimation was accomplished by quantifying nucleoli in characteristic cells in every fifth spinal cord section (every 100 μm in the rostral–caudal plane) from the entire lumbar spinal cord (Tomlinson and Irving 1977), for a total of six sections from each mouse. Counts included all apparent motor neurons including motor neurons that appeared atrophic or damaged in the field of view. Only neurons with a diameter greater than 50 μm for lumbar cord, and greater than 25 μm for thoracic spinal cord were included in the count (Cruz-Sanchez et al. 1998).

Statistical Analysis. For behavioral and histological experiments, individual measurements for each mouse were calculated as mean ± *SEM* for each group. The means were compared using an unpaired, two-tailed *t*-test or a one-way ANOVA. A *post hoc* Tukey's test was used to compare all means after ANOVA (GraphPad Prism, San Diego, CA).

Results

In vitro Studies

We treated the NSC-34 cell line with BSSG for 3 days and observed a dose-dependent increase in cell death (Fig. 1a) as measured by the trypan blue exclusion test. BSSG treatment doubled the loss of cells up to about 10% (Fig. 1a). Some of these cells stained positively for activated caspase-3, indicating apoptosis as a mechanism of cell death. Surviving cells were observed to extend long processes with many "beaded" segments along their length (Ly et al. 2007). Treatment with 50 μM of BSSG for 3 days followed by Western blots showed a significant up-regulation of HSP 70, indicative of a cell stress response (Fig. 1b–c). Under the same conditions, the cells showed a significant loss of the heavy neurofilament subunit in the soluble fraction of the cell lysate (Fig. 1d–e) accompanied by an increase in expression in the beaded processes (Ly et al. 2007).

In vivo Experiment Studies

Experiment 1

BSSG Blood Levels: The blood of BSSG-fed animals had significantly increased sterol glucoside serum levels (66%; Student's *t*-test) compared to controls with the control group showing more variability in total values (Fig. 2).

Behavioral Tests: Mice were tested for open field exploratory behavior a few weeks prior to sacrifice. Both groups showed a tendency for a decrease in open field activity during the testing period, but inter group differences were not statistically significant. BSSG-fed mice showed a significant decrease (−40%; Student's *t*-test) in overall movement as measured by grid crossing at week 28 (from start of feeding) (Fig. 3a).

BSSG-fed mice showed a progressive decrease on the leg extension test that became significant after week 30 compared to controls (Fig. 3b). As in our previous studies using cycad, the decline in leg extension was not a simple monotonic decline, but rather showed periods of increasing deficit followed by short-term recovery toward control values (Wilson et al. 2002). In contrast to the leg extension test which is the most sensitive for α-motor neuron loss or dysfunction, no significant motor deficits were observed for the rotorod, paw print, or wire hang tests.

CNS Pathology: *Motor neurons*. Nissl staining of BSSG-fed mice spinal cord showed a significant decrease in the number of large α-motor neurons in both the lumbar (−35%; Student's *t*-test) and thoracic (−19%; Student's *t*-test) spinal cord compared to controls (Fig. 4a). Further, some surviving motor neurons of BSSG-fed mice at both levels showed abnormal morphological features with surviving motor neurons showing shrunken somata with intense Nissl labelling (Fig. 4b–f), indiscrete nuclei (pyknotic) (dotted arrows). Other cells had large and disrupted membranes (solid arrows) indicative of chromatolysis. The appearances and the numbers of motor neurons were the same on both sides of the cord.

Anti-ChAT labelling of cholinergic neurons in lumbar spinal cord sections (Fig 5a–c) served as a complementary measurement to Nissl motor neuron counts with the numbers of large ChAT-positive cells with a distinct nucleus in the lateroventral horns of L2–L5 segments of the spinal cord being determined. ChAT labelling of motor neurons was significantly decreased in BSSG-fed mice compared to controls (−58%, Student's *t*-test). As shown above in Fig. 4, ChAT-positive labelled cells of BSSG-fed mice also showed abnormal morphological features compared to controls (Fig. 5c). Nissl motor neuron counts and ChAT positive labelling correlated remarkably well (−35%, −40%, respectively), strongly suggesting that most of the

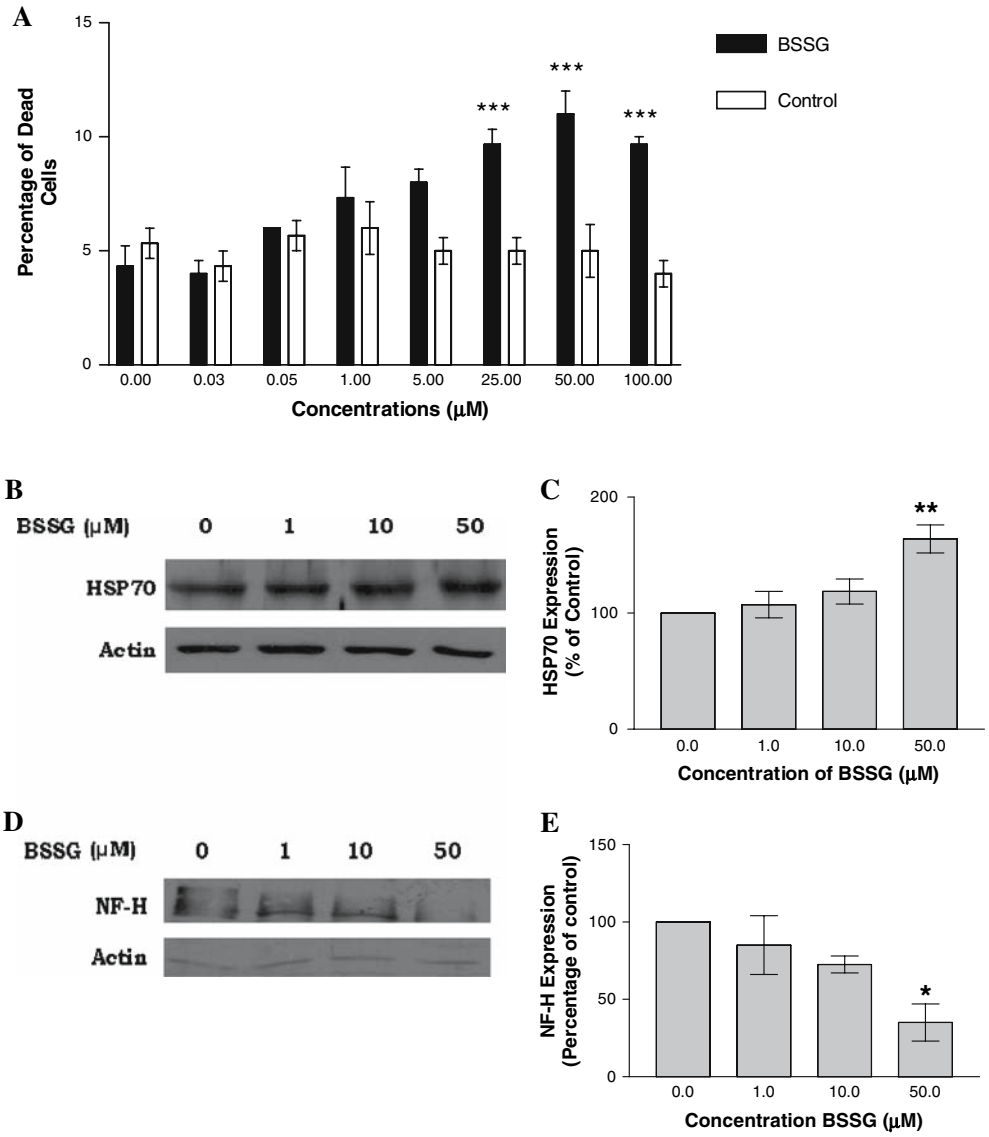

Fig. 1 In vitro dose-dependent toxicity and expression of HSP70 and heavy neurofilament (NF-H) after BSSG treatment. (**a**) NSC-34 cells (a motor neuron-derived cell line) were treated with increasing doses of BSSG. Cell death assays demonstrated BSSG dose-dependant toxicity. One-way analysis of variance (ANOVA) (*** $P < 0.001$) indicated a significant increase in cell death compared to controls. (**b**) Western blot analysis of HSP70 expression in NSC34 cells after treatment with increasing doses of BSSG (0, 1, 10, 50 μM). (**c**) Quantified results from the western blot show that the level of HSP70 expression increased after BSSG treatment, with 50 μM of BSSG inducing roughly a 50% over-expression (ANOVA, ** $P < 0.01$). (**d**) Western blot analysis of NF-H expression in NSC-34 cells after treatment with increasing doses of BSSG as in (**b**). (**e**) Quantified results from the Western blot show that the level of NF-H expression significantly decreased in the soluble fraction after 50 μM of BSSG treatment (ANOVA, * $P < 0.05$)

cell loss measured by the Nissl stain reflected the loss of motor neurons.

To determine the mechanism of cell death, we measured apoptosis with anti-active caspase-3 labelling. Examination of the lateroventral horns of L2–L5 (Fig. 5d–f) showed increased labelling in the ventral horn of the lumbar spinal cord (+200%) and in the striatum (+48%) of BSSG-fed mice compared to controls. In the cord, the morphology of the cells undergoing apoptosis confirmed that these were motor neurons (Fig. 5e).

Glial Response. The number of astrocytes was determined by counting GFAP-positive cells with star-shaped cell bodies in the lateroventral horns of L2–L5 segments of the spinal cord (Fig. 6a). BSSG-fed mice had significantly increased levels of activated astrocytes (+82%) that had characteristically larger and more ramified morphology (Fig. 6b–c). When the level of microglial infiltration was examined with Iba-1 labelling, BSSG-fed mice were found to have a greater number of microglia (+89%), although these data did not achieve statistical significance.

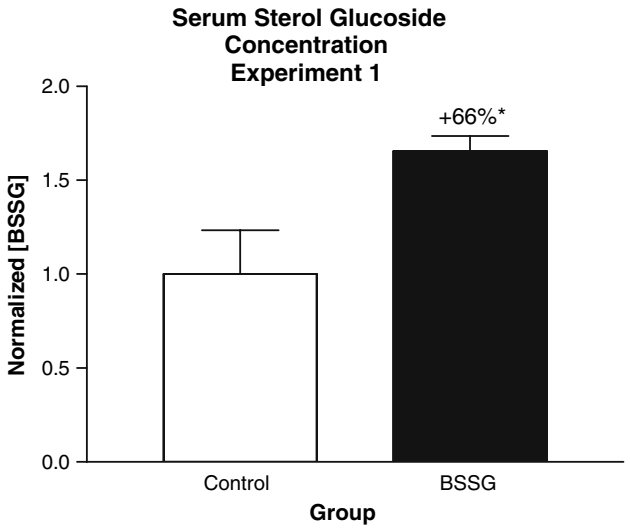

Fig. 2 Sterol glucoside serum concentrations. TLC analysis shows normalized (to control) sterol glucoside levels in blood collected at baseline and during the feeding paradigm. BSSG-fed mice (Experiment 1) showed significantly increased serum levels of sterol glucosides compared to controls (Student's *t*-test, * $P < 0.05$)

Glutamate Transporter. GLT-1B labelling (equivalent to the EAAT2 transporter) in the ventral horn of the lumbar spinal cord (Fig. 7a–d) of BSSG-fed mice showed a significant decrease in overall labelling (−18%). Several examples illustrating the range of the decrease in labelling in BSSG-fed mice are shown (Tzingounis et al. 1998).

Cell Proliferation: PCNA labelling of the lateroventral horn of the subventricular zone (Fig. 7a–c). PCNA labelling was significantly decreased (−40%) in BSSG-fed animals (Fig. 8).

Nigo-striatal Pathway: Mouse anti-tyrosine hydroxylase labelling of dopaminergic neurons in the striatum and SN (Fig. 9e–f) showed that BSSG-fed mice had significantly decreased TH labelling in the striatum (−13%) and in the SNpc (−12%) compared to controls.

Experiment 2

Motor Tests: No significant motor deficits were observed throughout this experiment in any of the groups fed BSSG compared to controls as determined by tests of leg extension, open field behavior, rotorod, paw print, or wire hang tests (data not shown).

CNS Pathology: Motor neuron counts in lumbar spinal cord using Nissl staining at time point 1 (10 weeks of feeding; 2 weeks post feeding) showed that mice fed BSSG had significantly fewer motor neurons (−34%) compared to controls in the treatment group receiving the highest dose (1,000 μg/day) (Fig. 10a, b). Counts from the second time point (22 weeks after last dose) showed that all three

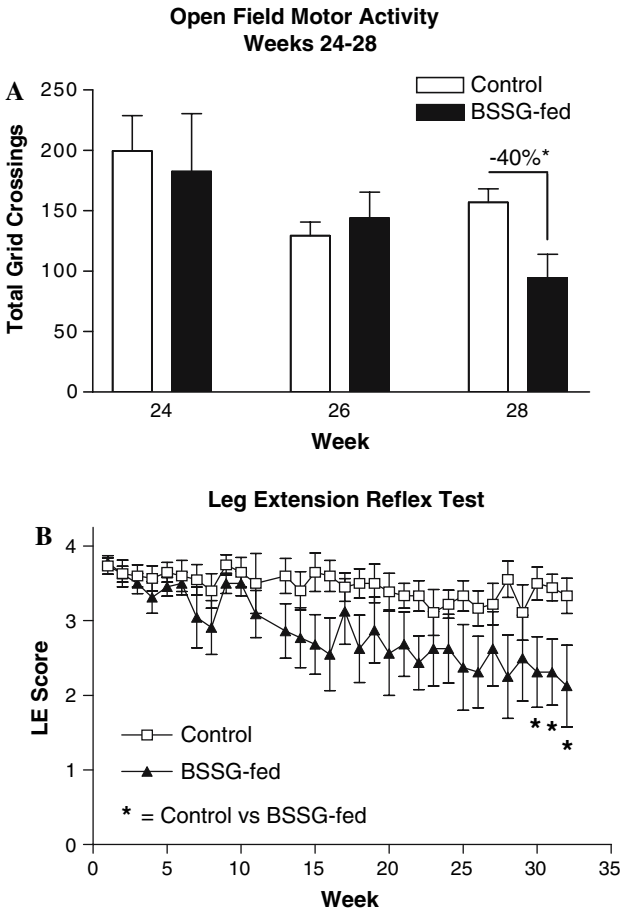

Fig. 3 Behavioral motor tests during BSSG treatment. (**a**) Open field motor activity. BSSG-fed mice showed significantly decreased movement as measured by grid crossing at week 28 compared to controls. (**b**) Leg extension (LE) measurements indicate an increasing motor defect. BSSG-fed mice showed a progressively decreasing score on the LE test that became significant after week 30 compared to controls. (**a**–**b**) Student's *t*-test, * $P < 0.05$

BSSG dosage groups had significantly decreased motor neurons counts compared to controls (10 μg: −33%; 100 μg: −31%; 1,000 μg: −44%) (Fig. 10a, b). Analysis of apoptosis, GLT-1B loss, and GFAP and Iba-1 labelling did not reveal significant differences in BSSG-fed mice, unlike in Experiment 1.

Discussion

The results of the present study confirm that BSSG can be neurotoxic in vitro and further suggest a novel in vivo pathology. In NSC-34 cells, BSSG treatment induced some cell death by apoptosis and was accompanied by up-regulated HSP70 expression and decreased cytosolic heavy neurofilament expression. These in vitro data reported here are consistent with our previous studies using mouse and human primary cortical cell cultures (Khabazian et al.

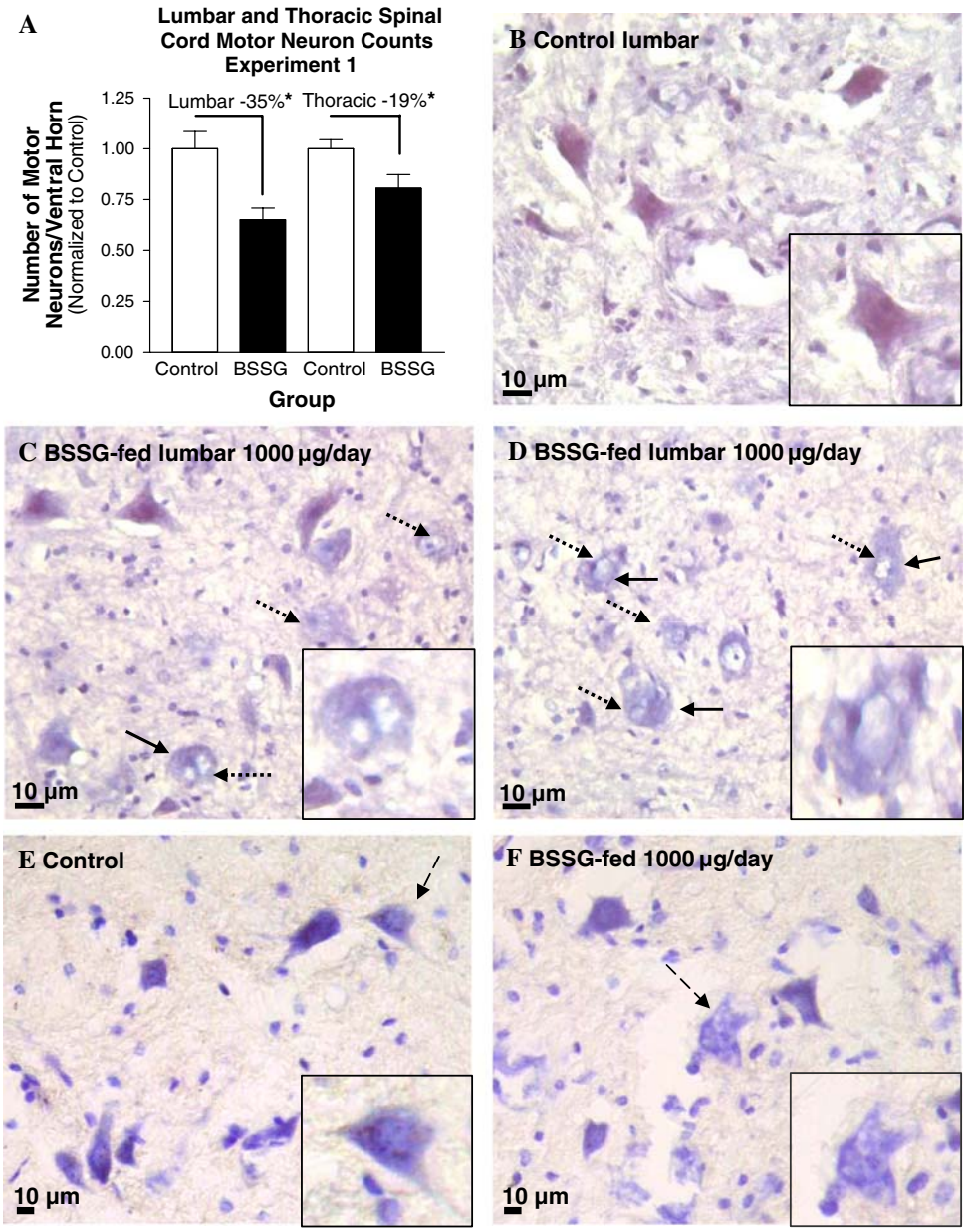

Fig. 4 Motor neuron counts following BSSG treatment. Experiment 1: CD-1 mice fed 1,000 µg of BSSG/day for 15 weeks. Mice were sacrificed and lumbar and thoracic spinal cord motor neuron counted 17 weeks later. (**a**) Lumbar and thoracic spinal cord motor neuron counts; *t*-test, * $P < 0.05$; (**b**–**d**). Normal (Control) and abnormal (BSSG-fed) motor neuron morphology visualized with cresyl violet (nissl body) staining in the lumbar spinal cord. (**e**, **f**) Cresyl violet staining in the thoracic spinal cord of a Control and BSSG-fed animal. Scale bars, all panels = 10 µm

2002) and the ongoing studies of organotypic slices of SN, striatum, hippocampus, and spinal cord (Wilson and Shaw 2006). More detailed studies of the overall effects of BSSG and other sterol glucosides and the time course of events are in progress. The data presented here demonstrate that an HSP response is involved as a relatively early event, mirroring a previous study showing that CG was involved in the HSP signaling pathway in response to cellular stress (Kunimoto et al. 2000). Whether HSP expression in the present experiments is a cellular attempt to provide protection, or if it reflects a part of the pathological process leading to cell death, or both, remains unresolved.

BSSG-treated animals showed significant increases in serum sterol glucoside levels at the various time points tested (Fig. 2). However, how these molecules might be transported into and out of the CNS remains unknown. In mammals greater than 95% of the total cholesterol in the brain is synthesized in situ with little uptake of cholesterol from plasma (Edmond et al. 1991; Jurevics and Morell 1995). Our detection of sterol glucosides in plasma accompanied by the resulting neuropathology may suggest that the glucose moiety confers greater transport capability into CNS. Alternatively, a metabolite of BSSG may be the toxic factor.

The crucial step in excreting excess cholesterol synthesized in the brain is by conversion to 24(S)-hydroxycholesterol, which, unlike cholesterol, can easily cross the blood–brain barrier (Lutjohann et al. 1996).

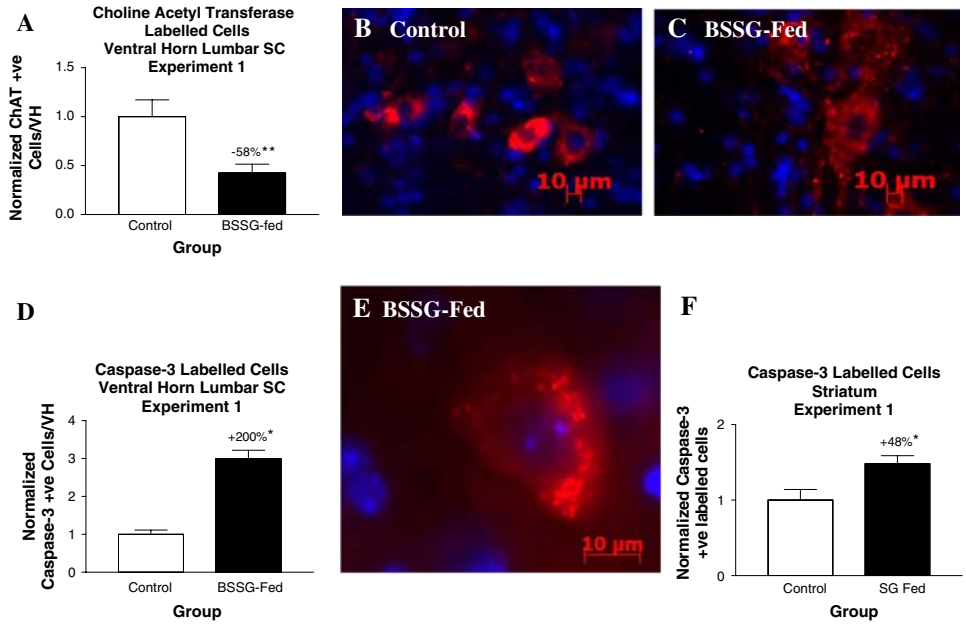

Fig. 5 ChAT and caspase-3 labelling in the brain and spinal cord of BSSG treated mice. (**a**) Quantification of ChAT labelling in the ventral horn of the lumbar spinal cord (*t*-test, ** $P < 0.01$). (**b–c**). Photomicrographs of ChAT labelled cells (red) in control and BSSG-fed mice. The blue label is DAPI. (**d**, **e**). Active caspase-3 labelling in the ventral horn of the lumbar spinal cord of control and BSSG-fed mice, respectively. In (**d**) active caspase-3 labelling is significantly increased in the ventral horn (*t*-test, * $P < 0.05$). (**e**) Photomicrograph of active caspase-3 labelled cells (red) in the spinal cord of BSSG-fed mice. Several examples are provided. Scale bars, all panels = 10 µm

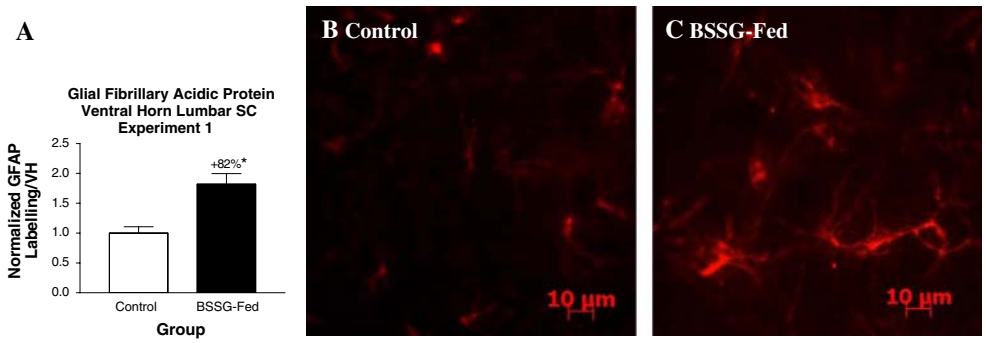

Fig. 6 Activated astrocytes in the ventral horn of the lumbar spinal cord of BSSG treated mice. (**a**) Quantification of GFAP labelling in the ventral horn of the lumbar spinal cord in control and BSSG-fed mice. BSSG-fed mice showed significantly increased GFAP labelled cells compared to the controls (Student's *t*-test, * $P < 0.05$). (**b**) Photomicrograph highlighting the lack of GFAP labelled cells in the ventral horn of the spinal cord of control mice; the blue label is DAPI. Scale bars, all panels = 10 µm. (**c**) Photomicrograph of GFAP labelled cells (red) in the ventral horn of the spinal cord of BSSG-fed mice

Roughly two-thirds of excess cholesterol is removed from the brain in this manner; the fate of the remainder is uncertain. We note that given the rapidity with which cholesterol is excreted (Quan et al. 2003), the levels of sterol glucoside in the serum of our treated mice may not reflect the overall chronic levels achieved in these experiments. It is also of interest that increased hydroxycholesterol has been described for Alzheimer's disease (Lutjohann et al. 2000; Papassotiropoulos et al. 2000; Heverin et al. 2004; Bjorkhem 2006). Whether the same is true in mice treated with sterol glucosides needs to be determined.

The initial in vivo experiments performed in this study (Experiment 1) were designed to test the hypothesis that BSSG in vivo will induce the same pathological events as those we have previously observed with cycad seed flour. The results show that at the single dose of 1,000 µg/day for 15 weeks CD-1 mice exhibit leg extension deficits beginning at week 28. In the lumbar spinal cord, motor neuron loss was accompanied by the loss of ChAT with both decreased to a similar extent (Figs. 4a; 5a). The ventral horn of the thoracic spinal cord also exhibited significant motor neuron loss, but to a lesser degree compared to the lumbar portion (Fig. 4a–f). Other pathological markers

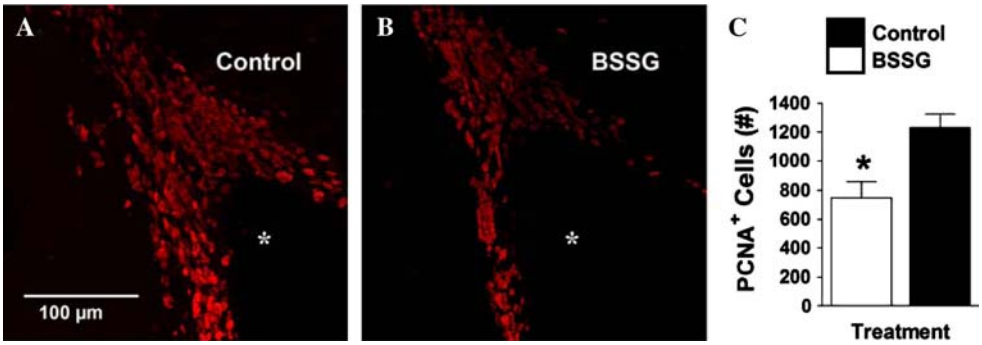

Fig. 7 Proliferating cell nuclear antigen (PCNA) in the lateroventral horn of the lumbar spinal cord of BSSG treated mice. (**a**, **b**) Representative fluorescent photomicrographs depicting immunolabeling of PCNA in the subventricular zone (SVZ) of control (**a**) and BSSG-fed (**b**) animals. Asterisk depicts the lateral ventricle. Scale bar = 100 µm. (**c**) Quantitative analysis of PCNA-positive cells in the SVZ. The number of PCNA-positive cells in the SVZ was significantly reduced following BSSG feeding. Each bar represents the mean (±*SEM*, $n = 4$) number of PCNA-positive cells counted in the SVZ. * $P < 0.05$

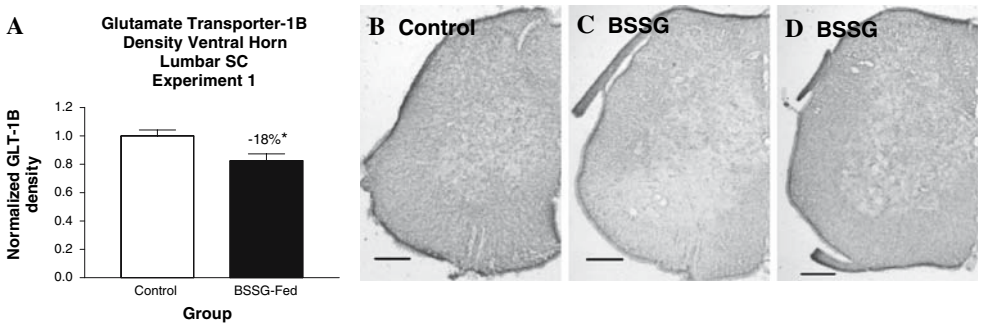

Fig. 8 Glutamate transporter 1B (GLT-1B) in the ventral horn of the lumbar spinal cord of BSSG treated mice. (**a**) GLT-1B labelling density in the ventral horn of the lumbar spinal cord. GLT-1B labelling is significantly decreased in BSSG-fed mice (Student *t*-test, * $P < 0.05$). Photomicrographs of GLT-1B labelled spinal cord sections: (**b**) Control. (**c–d**). BSSG-fed mice. BSSG-fed mice showed patchy loss of GLT-1B labelling primarily in the ventral horn of the spinal cord. (**b–d**) Scale bars = 1 mm

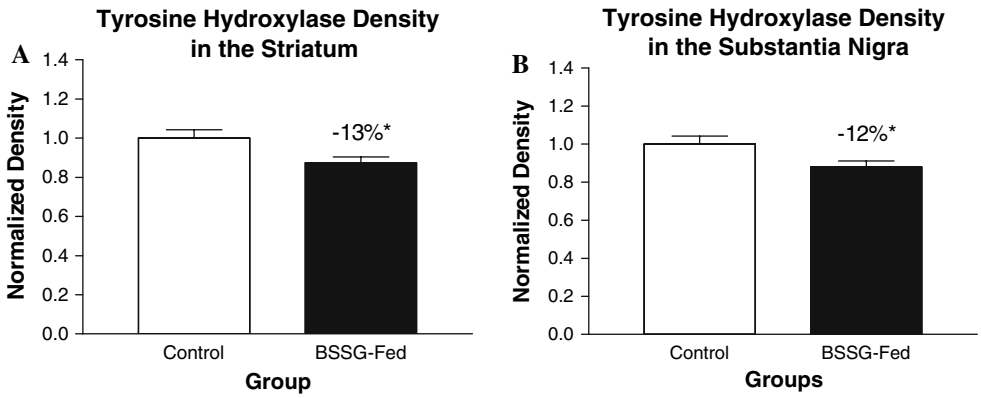

Fig. 9 Tyrosine hydroxylase labelling in the nigro-striatal region of BSSG treated mice. (**a–b**) Tyrosine hydroxylase (TH) in the striatum and SNpc. (**a**) Quantification of tyrosine hydroxylase labelling in the striatum. BSSG-fed mice (Experiment 1) showed significantly decreased tyrosine hydroxylase compared to the controls (*t*-test, * $P < 0.05$). (**b**) Quantification of tyrosine hydroxylase immunoreactive labelling in the SNpc. BSSG-fed mice showed significantly decreased tyrosine hydroxylase labelling compared to controls (*t*-test, * $P < 0.05$)

included an increase in active caspase-3 labelling indicative of increased apoptosis. The increase in apoptotic cell number (Fig. 5d, e) of BSSG-fed mice was greater than the level of loss of ChAT-labelled motor neurons (Fig. 5a–c), suggesting that dietary consumption of BSSG induces the degeneration of cell types other than motor neurons. This interpretation finds further support in the observation of increased caspase-3 labelling in the striatum (Fig. 5f).

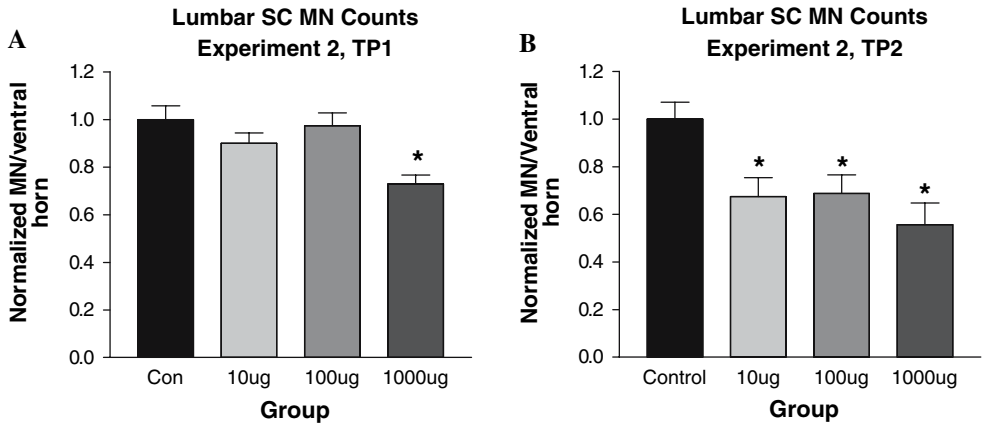

Fig. 10 Lumbar spinal cord motor neuron counts in BSSG treated mice. (**a**) Experiment 2, Time Point 1: C57/BL6 Mice fed 1000 μg of BSSG/day showed significantly decreased motor neuron counts compared to controls. (**b**) Experiment 2, Time Point 2: All 3 BSSG-fed groups showed significantly decreased motor neuron counts compared to controls. These results show that BSSG feeding induced a progressive neurodegeneration that was dose-dependent (One-way ANOVA, * $P < 0.05$)

The increased GFAP labelling of reactive astrocytes (Fig. 6a–c) confirms results previously reported with cycad flour feeding (Wilson et al. 2002, 2003, 2005b). Activated astrocytes were observed near both morphologically normal and abnormal motor neurons. In addition, the astrocytic processes in treated mice were longer and formed more complex networks. In human and mouse models of ALS, abundant gliosis is readily discernible in affected CNS regions (Kawamata et al. 1992; Hall et al. 1998; Sasaki and Iwata 1999; Anderson and Swanson 2000; Barbeito et al. 2004; Rao and Weiss 2004). The current data suggest a role for astrocytes in BSSG-induced neurotoxicity.

The increased microglial labelling observed in the present study also supports a role for a more general neuroinflammatory process in BSSG-induced neurotoxicity. This interpretation is supported by our ongoing studies using cycad flour that clearly demonstrate an increased microglial activation as one of the earliest pathological events in spinal cord (Lee et al. 2007).

It thus seems clear that both forms of glial activation can occur following exposure to cycad neurotoxins. Whether such events occur in sequence, in tandem, or transiently are not yet known. Indeed, there is considerable controversy in the experimental literature about the relative roles of astrocytes and microglia in neurodegeneration (Sargsyan et al. 2005).

Other pathological changes in the CNS of BSSG-treated mice included a decrease in GLT-1B labelling, suggestive of involvement of the glutamatergic system in the overall pathological processes underlying neurodegeneration (Fig. 7a–d). Again, this outcome mirrors results obtained in cycad fed mice and offers further evidence that BSSG recapitulates many of the overall pathological outcomes previously observed. Finally, the TH loss in striatum and SNpc, decreased cellular proliferation (PCNA) labelling in the subventricular zone, along with the increased caspase-3 labelling in striatum (Figs. 5f; 7a–c; 9e, f) are indicative of the involvement of the nigro-striatal system as is the case with cycad-fed mice (Wilson et al. 2002) and rats (Valentino et al. 2006).

Cumulatively, all of the observed changes in the lumbar spinal cord and the basal ganglia are consistent with many aspects of our cycad model of ALS–PDC, as well as with the disease itself (see Table 1). Work in progress is designed to examine other CNS regions involved in ALS–PDC in order to evaluate the extent of BSSG-induced neuropathology.

The second in vivo experiment conducted with C57/BL6 mice was designed to determine if the effects seen in Experiment 1 were strain specific and to provide a preliminary determination of the dose response relationship. The results demonstrated that strain specific outcomes occur following BSSG exposure that is similar to that following cycad feeding (Wilson et al. 2005a). Strain-dependent outcomes have also been noted for streptozotocin treatment (Sugimoto et al. 2007), hypoxia (Ward et al. 2007), exposure to cannabinoid receptor agonist (Hoffman et al. 2005), rinderpest virus (RPV), peste des petits ruminants virus (PPRV) (Galbraith et al. 2002), and naloxone (Navarro et al. 1991). Although no behavioral deficits were observed in our second in vivo study, there was significant motor neuron loss that was progressive with increasing survival times. Initial results (time point 1) showed that only the highest dose group (1,000 μg/day) gave significant outcomes. However, 5 months later (time point 2), all three dosage-groups showed significantly decreased motor neuron counts (Fig. 4f). Since no additional BSSG ingestion occurred during this time, these results suggest that BSSG-feeding induced a self-

Table 1 Summary of neurological outcomes following BSSG feeding in two in vivo experiments

	Experiment 1	Experiment 2	
		Timepoint 1	Timepoint 2
Mouse strain	CD1	C57/BL6	
Sex	Male	Male	
Numbers (*n*)	Control = 15; BSSG-fed = 16	Control = 14; 10 μg/day = 10; 100 μg/day = 10; 1,000 μg/day = 10	
BSSG feeding duration	15 weeks	10 weeks	
Washout period duration	17 weeks	2 weeks	22 weeks
Experiment duration	32 weeks	12 weeks	32 weeks
Behavioural tests	Open field motor activity* Leg extension*	ns	ns
Motor neurons per lumbar cord section	−35%*	1,000 μg: −30%*	10 μg: −33%* 100 μg: 31%* 1000 μg: −44%*
Motor neurons per thoracic cord section	−19%*	ns	ns
Choline acetyltransferase (ChAT)	−58%* (lumbar VH)	ns	ns
Proliferating cell nuclear antigen (PCNA)	−167%* (subventricular zone)		
Active caspase-3	+300%* (lumbar VH) + 148%* (striatum)	ns	ns
Glutamate transporter 1B (GLT-1B)	−18%* (lumbar VH)	ns	ns
Glial fibrillary acidic protein (GFAP)	+175%* (lumbar VH)	–	–
Ionized calcium-binding adaptor molecule-1 (IBA-1)	ns	ns	ns
Tyrosine hydroxylase (TH)	−13%* (striatum), −12%* (substantia nigra)	ns	ns

* $P < 0.05$; ns = not significant

perpetuating neurodegenerative cascade that took longer to develop in the lower dosage groups. Another possibility is that BSSG was retained in the CNS and continued to exert a neurotoxic effect over time. Studies now in progress are designed to determine if such retention occurs.

The lack of behavioral deficits in Experiment 2 may initially appear to be at variance with the observed significant loss of motor neurons. However, the notion that a large percentage of motor neurons must die before a behavioral deficit is apparent has been previously noted in the human neurodegenerative disease literature (Whitehouse et al. 1982). For example, by the time clinical diagnosis is achieved, major damage has been done to the most affected specific region(s) of the nervous system in various disorders. Estimates of neuron loss vary, but may be extensive in ALS (e.g., 70% loss of functional spinal alpha motor neurons (Arasaki and Tamaki 1998)); in Alzheimer's disease, greater than 75% loss of neurons of the nucleus basalis of Meynert may occur before disease onset (Whitehouse et al. 1982); similarly, in Parkinson's disease approximately 60–90% of dopamine-containing neurons in the SN are apparently lost (Piggott et al. 1999) before clinical features become evident. In all of the above disorders, redundant neuronal circuits and even compensatory mechanisms by surviving neurons may sustain the pre-clinical status over prolonged periods, at least until a final threshold of functional neuronal loss has occurred. If this interpretation is correct, behavioral deficits may become detectable only after severe damage beyond this threshold has been reached. The differential outcome in both overall pathology and behavioral deficits observed in the two in vivo studies reported here may reflect different thresholds between the two murine strains.

Overall, the data from the two in vivo experiments (Table 1) show that BSSG is neurotoxic to motor neurons with fewer non-motor neuron neural populations affected than previously observed in cycad-fed mice at equivalent time points with both mouse strains (Wilson et al. 2002, 2003, 2004a, b, 2005b). This outcome may suggest that BSSG alone is not sufficient to fully replicate the widespread behavioral deficits and pathology seen in cycad-fed mice or in ALS–PDC. In regard to this point, we note that Khabazian et al. (2002) showed that cycad contains three primary neurotoxic sterol glucoside variants: BSSG, campesterol β-D-glucoside, and stigmasterol β-D-glucoside. Both of the latter molecules were also acutely toxic in vitro, with the level of toxicity up to 100 times greater than that of BSSG (Khabazian et al. 2002). Thus, in washed

cycad flour, all three of these sterol glucoside molecules might synergistically operate to generate the overall ALS–PDC phenotype. Another possibility is that the each of the cycad sterol glucosides may have differential neurotoxic actions on the various neuronal populations that depend on either access to the CNS and/or the still unknown type(s) of binding site for these molecules. Evidence that access may be crucial comes from two observations. First, as cited in the Introduction, all cells affected in ALS–PDC can be killed by BSSG in cell culture preparations. Secondly, at the late time point in Experiment 1, early signs of nigrostriatal damage were beginning to appear.

How might identified cycad toxins be involved in neurodegenerative diseases other than ALS–PDC? One answer is that other sources of the putative sterol glucoside neurotoxins must exist in the environment. In relation to this point, the literature shows that phytosterol glucosides and cholesterol glucoside can arise from various sources including diet (Ly et al. 2007). For example, soy products containing phytosterols and phytosterol glucosides are major components of the human diet for some populations (Sugiyama and Seki 1991; Kawano et al. 2002; Maitani et al. 1995; Shimizu et al. 1997). A second potential source is by autosynthesis in which human cells may make sterol glucosides if the substrates of sterols and glucose are present. The synthesis of such molecules presumably depends on enzymes similar in function to sterol glucosyltransferase (Warnecke et al. 1997). Evidence that such synthesis of sterol glucosides can occur in human cells has been demonstrated for human fibroblasts in culture following heat shock (Kunimoto et al. 2000, 2002) and recently in our laboratory by serum derprivation (Ly et al. in preparation). A third source may involve infectious agents. For example, CG is a cell wall component of several forms of bacteria including *Candida bogoriensis* (Kastelic-Suhadolc 1980) and *Helicobacter pylori* (Hirai et al. 1995; Nicolson et al. 2002; Chapman et al. 2003) amongst others. *H. pylori* infections are positively correlated with an increased risk for Parkinson's disease (Dobbs et al. 2000).

Finally, we note that both in our cycad studies and now in our work with BSSG we have been able to provide a preliminary time line of the pathological events. The ability to induce a clear temporal sequence of behavioral and pathological changes in the CNS may provide important clues to the overall process of neurodegeneration. If such data could be correlated to the still unknown stages in human neurological disease, they might provide a wealth of pharmacological targets for early therapeutic intervention.

Acknowledgments This work was supported by grants from the ALS Association, the Scottish Rite Charitable Foundation of Canada, the Natural Science and Engineering Research Council of Canada, and the US Army Medical Research and Materiel Command (#DAMD17-02-1-0678) to C.A.S and from the Canadian Institutes of Health Research (CIHR) and PrioNet to N.C. The GLT-1B antibodies were kindly donated by Dr. D. Pow (University of Newcastle). Drs. R. Cruz-Aguado, D.G. Kay and I.E.P. Taylor and M. Petrik provided helpful critiques of earlier drafts of the manuscript.

References

Anderson, C. M., & Swanson, R. A. (2000). Astrocyte glutamate transport: Review of properties, regulation, and physiological functions. *Glia, 32*, 1–14.

Arasaki, K., & Tamaki, M. (1998). A loss of functional spinal alpha motor neurons in amyotrophic lateral sclerosis. *Neurology, 51*, 603–605.

Barbeito, L. H., Pehar, M., Cassina, P., Vargas, M. R., Peluffo, H., Viera, L., Estevez, A. G., & Beckman, J. S. (2004). A role for astrocytes in motor neuron loss in amyotrophic lateral sclerosis. *Brain Research Brain Research Reviews, 47*, 263–274.

Barneoud, P., & Curet, O. (1999). Beneficial effects of lysine acetylsalicylate, a soluble salt of aspirin, on motor performance in a transgenic model of amyotrophic lateral sclerosis. *Experimental Neurology, 155*, 243–251.

Barneoud, P., Lolivier, J., Sanger, D. J., Scatton, B., & Moser, P. (1997). Quantitative motor assessment in FALS mice: A longitudinal study. *Neuroreport, 8*, 2861–2865.

Bjorkhem, I. (2006). Crossing the barrier: Oxysterols as cholesterol transporters and metabolic modulators in the brain. *Journal of Internal Medicine, 260*, 493–508.

Borenstein, A. R., Mortimer, J. A., Schofield, E., Wu, Y., Salmon, D. P., Gamst, A., Olichney, J., Thal, L. J., Silbert, L., Kaye, J., Craig, U. L., Schellenberg, G. D., & Galasko, D. R. (2007). Cycad exposure and risk of dementia, MCI, and PDC in the Chamorro population of Guam. *Neurology, 68*, 1764–1767.

Buenz, E. J, & Howe, C. L. (2007). Beta-methylamino-alanine (BMAA) injures hippocampal neurons in vivo. *Neurotoxicology, 28*, 702–704.

Chapman, G., Beaman, B. L., Loeffler, D. A., Camp, D. M., Domino, E. F., Dickson, D. W., Ellis, W. G., Chen, I., Bachus, S. E., & LeWitt, P. A. (2003). In situ hybridization for detection of nocardial 16S rRNA: Reactivity within intracellular inclusions in experimentally infected cynomolgus monkeys–and in Lewy body-containing human brain specimens. *Experimental Neurology, 184*, 715–725.

Cruz-Aguado, R., Winkler, D., & Shaw, C. A. (2006). Lack of behavioral and neuropathological effects of dietary b-methylaminoalanine (BMAA) in mice. *Pharmacology, Biochemistry, and Behavior, 84*, 294–299.

Cruz-Sanchez, F. F., Moral, A., Tolosa, E., de Belleroche, J., & Rossi, M. L. (1998). Evaluation of neuronal loss, astrocytosis and abnormalities of cytoskeletal components of large motor neurons in the human anterior horn in aging. *Journal of Neural Transmission, 105*, 689–701.

Dobbs, S. M., Dobbs, R. J., Weller, C., & Charlett, A. (2000). Link between *Helicobacter pylori* infection and idiopathic parkinsonism. *Medical Hypotheses, 55*, 93–98.

Edmond, J., Korsak, R. A., Morrow, J. W., Torok-Both, G., & Catlin, D. H. (1991). Dietary cholesterol and the origin of cholesterol in the brain of developing rats. *Journal of Nutrition and Dietetics, 121*, 1323–1330.

Folmer, B. M. (2003). Sterol surfactants: From synthesis to applications. *Advances in Colloid and Interface Science, 103*, 99–119.

Galasko, D., Salmon, D., Gamst, A., Olichney, J., Thal, L. J., Silbert, L., Kaye, J., Brooks, P., Adonay, R., Craig, U. K., Schellenberg, G., & Borenstein, A. R. (2007). Prevalence of dementia in Chamorros on Guam: Relationship to age, gender, education, and APOE. *Neurology, 68*, 1772–1781.

Galbraith, S. E., McQuaid, S., Hamill, L., Pullen, L., Barrett, T., & Cosby, S. L. (2002). Rinderpest and peste des petits ruminants viruses exhibit neurovirulence in mice. *Journal of Neurovirology, 8*, 45–52.

Gerlai, R., Millen, K. J., Herrup, K., Fabien, K., Joyner, A. L., & Roder, J. (1996). Impaired motor learning performance in cerebellar En-2 mutant mice. *Behavioral Neuroscience, 110*, 126–133.

Gerlai, R., Roder, J. (1996). Spatial and nonspatial learning in mice: Effects of S100 beta overexpression and age. *Neurobiology of Learning and Memory, 66*, 143–154.

Grunwald, C. (1980) Steroids. In *Encyclopedia of plant physiology*. New series. Secondary plant products, Vol. 8, p. 221.

Hall, E. D., Oostveen, J. A., & Gurney, M. E. (1998). Relationship of microglial and astrocytic activation to disease onset and progression in a transgenic model of familial ALS. *Glia, 23*, 249–256.

Heverin, M., Bogdanovic, N., Lutjohann, D., Bayer, T., Pikuleva, I., Bretillon, L., Diczfalusy, U., Winblad, B., & Bjorkhem, I. (2004). Changes in the levels of cerebral and extracerebral sterols in the brain of patients with Alzheimer's disease. *Journal of Lipid Research, 45*, 186–193.

Hirai, Y., Haque, M., Yoshida, T., Yokota, K., Yasuda, T., & Oguma, K. (1995). Unique cholesteryl glucosides in *Helicobacter pylori*: Composition and structural analysis. *Journal of Bacteriology, 177*, 5327–5333.

Hoffman, A. F., Macgill, A. M., Smith, D., Oz, M., & Lupica, C. R. (2005). Species and strain differences in the expression of a novel glutamate-modulating cannabinoid receptor in the rodent hippocampus. *The European Journal of Neuroscience, 22*, 2387–2391.

Jurevics, H., & Morell, P. (1995). Cholesterol for synthesis of myelin is made locally, not imported into brain. *Journal of Neurochemistry, 64*, 895–901.

Karl, T., Pabst, R., & von Horsten, S. (2003). Behavioral phenotyping of mice in pharmacological and toxicological research. *Experimental and Toxicologic Pathology, 55*, 69–83.

Kastelic-Suhadolc, T. (1980). Cholesteryl glucoside in *Candida bogoriensis*. *Biochimica et Biophysica Acta, 620*, 322–325.

Kawamata, T., Akiyama, H., Yamada, T., & McGeer, P. L. (1992). Immunologic reactions in amyotrophic lateral sclerosis brain and spinal cord tissue. *American Journal of Pathology, 140*, 691–707.

Kawano, K., Nakamura, K., Hayashi, K., Nagai, T., Takayama, K., & Maitani, Y. (2002). Liver targeting liposomes containing beta-sitosterol glucoside with regard to penetration-enhancing effect on HepG2 cells. *Biological and Pharmaceutical Bulletin, 25*, 766–770.

Khabazian, I., Bains, J. S., Williams, D. E., Cheung, J., Wilson, J. M., Pasqualotto, B. A., Pelech, S. L., Andersen, R. J., Wang, Y. T., Liu, L., Nagai, A., Kim, S. U., Craig, U. K., & Shaw, C. A. (2002). Isolation of various forms of sterol beta-D-glucoside from the seed of *Cycas circinalis*: Neurotoxicity and implications for ALS-parkinsonism dementia complex. *Journal of Neurochemistry, 82*, 516–528.

Kunimoto, S., Kobayashi, T., Kobayashi, S., & Murakami-Murofushi, K. (2000). Expression of cholesteryl glucoside by heat shock in human fibroblasts. *Cell Stress and Chaperones, 5*, 3–7.

Kunimoto, S., Murofushi, W., Kai, H., Ishida, Y., Uchiyama, A., Kobayashi, T., Kobayashi, S., Murofushi, H., & Murakami-Murofushi, K. (2002). Steryl glucoside is a lipid mediator in stress-responsive signal transduction. *Cell Structure and Function, 27*, 157–162.

Kurland, L. T. (1972). An appraisal of the neurotoxicity of cycad and the etiology of amyotrophic lateral sclerosis on Guam. *Federation Proceedings, 31*, 1540–1542.

Kurland, L. T., & Molgaard, C. A. (1982). Guamanian ALS: Hereditary or acquired? *Advances in Neurology, 36*, 165–171.

Kurland, L. T. (1988). Amyotrophic lateral sclerosis and Parkinson's disease complex on Guam linked to an environmental neurotoxin. *Trends in Neuroscience, 11*, 51–54.

Lee, G., Cruz-Aguado, R., Banjo, O. C., & Shaw, C. A. (2007). Characterization of gait analysis, memory, and neuromuscular junction integrity in a mouse model of ALS–PDC. In *Neuroscience meeting planner*. San Diego, CA: Society for Neuroscience.

Lutjohann, D., Breuer, O., Ahlborg, G., Nennesmo, I., Siden, A., Diczfalusy, U., & Bjorkhem, I. (1996). Cholesterol homeostasis in human brain: Evidence for an age-dependent flux of 24S-hydroxycholesterol from the brain into the circulation. *Proceedings of the National Academy of Sciences of the United States of America, 93*, 9799–9804.

Lutjohann, D., Papassotiropoulos, A., Bjorkhem, I., Locatelli, S., Bagli, M., Oehring, R. D., Schlegel, U., Jessen, F., Rao, M. L., von Bergmann, K., & Heun, R. (2000). Plasma 24S-hydroxycholesterol (cerebrosterol) is increased in Alzheimer and vascular demented patients. *Journal of Lipid Research, 41*, 195–198.

Ly, P. T., Singh, S., & Shaw, C. A. (2007). Novel environmental toxins: Steryl glycosides as a potential etiological factor for age-related neurodegenerative diseases. *Journal of Neuroscience Research, 85*, 231–237.

Maitani, Y., Hazama, M., Tojo, H., Qi, X. R., & Nagai, T. (1995). Effects of orally administered liposomes with soybean-derived sterols and their glucosides on rat body weight. *Biological and Pharmaceutical Bulletin, 18*, 1551–1555.

Marler, T., Lee, V., & Shaw, C. A. (2005). Cycad toxins and neurological diseases in Guam: Defining theoretical experimental standards for correlating human disease with environmental toxins. *Horticultural Science, 40*, 1607–1611.

Marler, T. E., Lee, V., Chung, J., & Shaw, C. A. (2006). Steryl glucoside concentration declines with *Cycas micronesica* seed age. *Functional Plant Biology, 33*, 857–862.

Miettinen, T. A., Alfthan, G., Huttunen, J. K., Pikkarainen, J., Naukkarinen, V., Mattila, S., & Kumlin, T. (1983) Serum selenium concentration related to myocardial infarction and fatty acid content of serum lipids. *British Medical Journal (Clinical Research Ed.), 287*, 517–519.

Morrow, C. E., Bandstra, E. S., Anthony, J. C., Ofir, A. Y., Xue, L., & Reyes, M. L. (2001). Influence of prenatal cocaine exposure on full-term infant neurobehavioral functioning. *Neurotoxicology and Teratology, 23*, 533–544.

Murakami-Murofushi, K., Nishikawa, K., Hirakawa, E., & Murofushi, H. (1997). Heat stress induces a glycosylation of membrane sterol in myxoamoebae of a true slime mold, *Physarum polycephalum*. *Journal of Biological Chemistry, 272*, 486–489.

Murch, S. J., Cox, P. A., & Banack, S. A. (2004). A mechanism for slow release of biomagnified cyanobacterial neurotoxins and neurodegenerative disease in Guam. *Proceedings of the National Academy of Sciences of the United States of America, 101*, 12228–12231.

Navarro, M., Leza, J. C., Lizasoain, I., & Lorenzo, P. (1991). Influence of psychogenetics in opiate tolerance and abstinence in mice. *General Pharmacology, 22*, 713–716.

Nesher, M., Shpolansky, U., Rosen, H., & Lichtstein, D. (2007). The digitalis-like steroid hormones: New mechanisms of action and biological significance. *Life Science, 80*, 2093–2107.

Nicolson, G. L., Nasralla, M. Y., Haier, J., & Pomfret, J. (2002). High frequency of systemic mycoplasmal infections in Gulf War veterans and civilians with amyotrophic lateral sclerosis (ALS). *Journal of Clinical Neuroscience, 9*, 525–529.

Papassotiropoulos, A., Lutjohann, D., Bagli, M., Locatelli, S., Jessen, F., Rao, M. L., Maier, W., Bjorkhem, I., von Bergmann, K., & Heun, R. (2000). Plasma 24S-hydroxycholesterol: A peripheral indicator of neuronal degeneration and potential state marker for Alzheimer's disease. *Neuroreport, 11*, 1959–1962.

Pegel, K. H. (1997). The importance of sitosterol and sitosterolin in human and animal nutrition. *South African Journal of Science, 93*, 263–268.

Perry, T. L., Bergeron, C., Biro, A. J., & Hansen, S. (1989). Beta-N-methylamino-L-alanine. Chronic oral administration is not neurotoxic to mice. *Journal of Neurological Science, 94*, 173–180.

Piggott, M. A., Marshall, E. F., Thomas, N., Lloyd, S., Court, J. A., Jaros, E., Burn, D., Johnson, M., Perry, R. H., McKeith, I. G., Ballard, C., & Perry, E. K. (1999). Striatal dopaminergic markers in dementia with Lewy bodies, Alzheimer's and Parkinson's diseases: Rostrocaudal distribution. *Brain, 122*(Pt 8), 1449–1468.

Quan, G., Xie, C., Dietschy, J. M., & Turley, S. D. (2003). Ontogenesis and regulation of cholesterol metabolism in the central nervous system of the mouse. *Brain Research Developmental Brain Research, 146*, 87–98.

Rao, S. D., & Weiss, J. H. (2004). Excitotoxic and oxidative cross-talk between motor neurons and glia in ALS pathogenesis. *Trends in Neuroscience, 27*, 17–23.

Reye, P., Sullivan, R., Scott, H., & Pow, D. V. (2002). Distribution of two splice variants of the glutamate transporter GLT-1 in rat brain and pituitary. *Glia, 38*, 246–255.

Ross, S. M., Roy, D. N., & Spencer, P. S. (1989). Beta-N-oxalylamino-L-alanine action on glutamate receptors. *Journal of Neurochemistry, 53*, 710–715.

Sanders, D. J., Minter, H. J., Howes, D., & Hepburn, P. A. (2000). The safety evaluation of phytosterol esters. Part 6. The comparative absorption and tissue distribution of phytosterols in the rat. *Food and Chemical Toxicology, 38*, 485–491.

Sargsyan, S. A., Monk, P. N., & Shaw, P. J. (2005). Microglia as potential contributors to motor neuron injury in amyotrophic lateral sclerosis. *Glia, 51*, 241–253.

Sasaki, S., & Iwata, M. (1999). Immunoreactivity of beta-amyloid precursor protein in amyotrophic lateral sclerosis. *Acta Neuropathology (Berl), 97*, 463–468.

Schulz, J. D., Khabazian, I., Wilson, J. M., & Shaw, C. A. (2003). A muring model of ALS-PDC with behavioural and neuropathological features of Parkinsonism. *Annals of the New York Academy of Sciences, 991*, 326–329.

Shimizu, K., Maitani, Y., Takayama, K., & Nagai, T. (1997). Formulation of liposomes with a soybean-derived sterylglucoside mixture and cholesterol for liver targeting. *Biological and Pharmaceutical Bulletin, 20*, 881–886.

Spencer, P. S., Ross, S. M., Nunn, P. B., Roy, D. N., & Seelig, M. (1987). Detection and characterization of plant derived amino acid motorsystem toxins in mouse CNS cultures. *Progress in Clinical and Biological Research, 253*, 349–361.

Sugimoto, H., Grahovac, G., Zeisberg, M., & Kalluri, R. (2007). Renal fibrosis and glomerulosclerosis in a new mouse model of diabetic nephropathy and its regression by BMP-7 and advanced glycation end-product inhibitors. *Diabetes, 56*(7), 1825–1833.

Sugiyama, M., & Seki, J. (1991). In vivo application of lipoproteins as drug carriers: Pharmacological evaluation of sterylglucoside-lipoprotein complexes. *Targeted Diagnosis and Therapy, 5*, 315–350.

Tomlinson, B. E., & Irving, D. (1977). The numbers of limb motor neurons in the human lumbosacral cord throughout life. *Journal of Neurological Sciences, 34*, 213–219.

Tzingounis, A. V., Lin, C. L., Rothstein, J. D., & Kavanaugh, M. P. (1998). Arachidonic acid activates a proton current in the rat glutamate transporter EAAT4. *Journal of Biological Chemistry, 273*, 17315–17317.

Valentino, K. M., Dugger, N. V., Peterson, E., Wilson, J. M., Shaw, C. A., & Yarowsky, P. J. (2006). Environmentally induced parkinsonism in cycad-fed rats. *Society for Neuroscience Abstract*.

Ward, N. L., Moore, E., Noon, K., Spassil, N., Keenan, E., Ivanco, T. L., & LaManna, J. C. (2007). Cerebral angiogenic factors, angiogenesis, and physiological response to chronic hypoxia differ among four commonly used mouse strains. *Journal of Applied Physiology, 102*, 1927–1935.

Warnecke, D. C., Baltrusch, M., Buck, F., Wolter, F. P., & Heinz, E. (1997). UDP-glucose: Sterol glucosyltransferase: Cloning and functional expression in *Escherichia coli*. *Plant Molecular Biology, 35*, 597–603.

Welsh, J. P., Yamaguchi, H., Zeng, X. H., Kojo, M., Nakada, Y., Takagi, A., Sugimori, M., & Llinas, R. R. (2005). Normal motor learning during pharmacological prevention of Purkinje cell long-term depression. *Proceedings of the National Academy of Sciences of the United States of America, 102*, 17166–17171.

Whitehouse, P. J., Price, D. L., Struble, R. G., Clark, A. W., Coyle, J. T., & Delon, M. R. (1982). Alzheimer's disease and senile dementia: Loss of neurons in the basal forebrain. *Science, 215*, 1237–1239.

Whiting, M. G. (1963). Toxicity of cycads. *Economic Botany, 17*, 271–302.

Wilson, J. M., Khabazian, I., Pow, D. V., Craig, U. K., & Shaw, C. A. (2003). Decrease in glial glutamate transporter variants and excitatory amino acid receptor down-regulation in a murine model of ALS-PDC. *Neuromolecular Medicine, 3*, 105–118.

Wilson, J. M., Khabazian, I., Wong, M. C., Seyedalikhani, A., Bains, J. S., Pasqualotto, B. A., Williams, D. E., Andersen, R. J., Simpson, R. J., Smith, R., Craig, U. K., Kurland, L. T., & Shaw, C. A. (2002). Behavioral and neurological correlates of ALS-parkinsonism dementia complex in adult mice fed washed cycad flour. *Neuromolecular Medicine, 1*, 207–221.

Wilson, J. M., Petrik, M. S., Blackband, S. J., Grant, S. C., & Shaw, C. A. (2003). Quantitative measurement of neurodegeneration in ALS-PDC model using MRI. *UBC Department of Ophthalmology Research Day Abstracts*. See copy included in application.

Wilson, J. M., Petrik, M. S., Grant, S. C., Blackband, S. J., Lai, J., & Shaw, C. A. (2004a). Quantitative measurement of neurodegeneration in an ALS-PDC model using MR microscopy. *Neuroimage, 23*, 336–343.

Wilson, J. M., Petrik, M. S., Moghadasian, M. H., & Shaw, C. A. (2005a). Examining the interaction of apo E and neurotoxicity on a murine model of ALS-PDC. *Canadian Journal of Physiology and Pharmacology, 83*, 131–141.

Wilson, J. M., Petrik, M. S., Moghadasian, M. H., Grant, S. C., Blackband, S. J., Krieger, C., Craig, U. K., & Shaw, C. A. (2005b). The progression of motor deficits and CNS pathology in ALS-PDC. *Society for Neuroscience Abstracts*. online.

Wilson, J. M., Petrik, M. S., Moghadasian, M. H., Grant, S. C., Blackband, S. J., Krieger, C., Craig, U. K., & Shaw, C. A. (2005c). The progression of motor deficits and CNS pathology in ALS-PDC. *Society for Neuroscience Abstracts.* online.

Wilson, J. M., Petrik, M. S., Rosebrugh, R. L., Moghadasian, M. H., & Shaw, C. A. (2004b). Dynamic interaction of gene and environment using APOE allele variants in an animal model of ALS-PDC. *Society for Neuroscience Abstracts*, 341.11.

Wilson, J. M., & Shaw, C. A. (2006). Late appearance of glutamate transporter defects in a murine model of ALS-parkinsonism dementia complex. *Neurochemsitry International, 50*, 1067–1077.